Rapid uplift of nonmethane hydrocarbons in a cold front over central Europe

R. M. Purvis,[1] A. C. Lewis,[1,2] R. A. Carney,[2] J. B. McQuaid,[2] S. R. Arnold,[2] J. Methven,[3] H. Barjat,[4] K. Dewey,[4] J. Kent,[4] P. S. Monks,[5] L. J. Carpenter,[6] N. Brough,[7] S. A. Penkett,[7] and C. E. Reeves[7]

[1] The vertical distribution of 21 C_2–C_7 nonmethane hydrocarbons (NMHCs) has been determined in planetary boundary layer (PBL) and free tropospheric (FT) air over central Europe under a range of meteorological conditions. High-frequency whole air sampling was conducted on board the U.K. Meteorological Office C-130 Hercules aircraft during the European Export of Precursors and Ozone by Long-Range Transport (EXPORT) experiment in August 2000. When vertical transport by large-scale flow or convection was weak, the expected large concentration gradient between the PBL and FT was observed for all short and medium lifetime hydrocarbons (e.g., average *iso*-butane, PBL 100 pptV, FT 6 pptV). During periods of strong convective activity associated with the passage of a cold front, a rapid uplift of reactive carbon from the boundary layer to the mid free troposphere was observed. Using changing ratios of hydrocarbons with different atmospheric lifetimes, a timescale for transport during this event was determined. Hydrocarbon lifetime measurements suggest that in certain regions of the system, it is convective transport embedded within the cold front rather than larger-scale advection along the warm conveyor belt that is dominant in transporting ozone precursors into the free troposphere. *INDEX TERMS:* 0317 Atmospheric Composition and Structure: Chemical kinetic and photochemical properties; 0341 Atmospheric Composition and Structure: Middle atmosphere—constituent transport and chemistry (3334); 0368 Atmospheric Composition and Structure: Troposphere—constituent transport and chemistry; *KEYWORDS:* nonmethane hydrocarbons, frontal systems, long-range transport, tropospheric ozone, convection

1. Introduction

[2] Nonmethane hydrocarbons (NMHCs) are released into the atmosphere from a diverse range of both anthropogenic and biogenic sources. They are removed from the atmosphere mainly during the daytime by reaction with hydroxyl radicals (OH), and in the presence of nitrogen oxides (NO_x) their oxidation leads to the formation of ozone. Once in the relatively dry upper troposphere, ozone itself has an enhanced photochemical lifetime allowing intercontinental transport and a proportionally greater influence on climate than at the surface [*Lacis et al.*, 1990]. Approximately 10% of atmospheric ozone resides in the free troposphere [*Intergovernmental Panel on Climate Change (IPCC)*, 1999], its content controlled by in situ photochemical production and destruction, direct exchange from the stratosphere or uplift of ozone from the boundary layer. Observations and modeling now support a mechanism of in situ ozone production over stratosphere-troposphere exchange (STE) as the primary source of tropospheric ozone [*Lelieveld and Denter*, 2000], where boundary layer air influences free tropospheric concentrations *via* direct exchange of ozone, or indirect transport of precursors necessary for its production.

[3] Mechanisms for transport of ozone from the stratosphere to the troposphere have been well documented [e.g., *Holton et al.*, 1995], and in early studies were considered to be the sole source of tropospheric ozone. In situ ozone production in the free troposphere is now however an established principle and has been shown to be highly efficient with respect to NO_x molecules consumed [e.g., *Carpenter et al.*, 2000]. The transfer of precursors necessary for this photochemical production across the boundary layer - free troposphere interface is less well understood. Within the planetary boundary layer over much of Europe, ozone production has been proposed as being limited by the availability of volatile organic compounds, of which NMHCs are a key subset [*U.K. Photochemical Oxidant*

[1]School of Chemistry, University of Leeds, Leeds, UK.
[2]School of the Environment, University of Leeds, Leeds, UK.
[3]Department of Meteorology, University of Reading, Reading, UK.
[4]U.K. Meteorological Office, Farnborough, UK.
[5]School of Chemistry, University of Leicester, Leicester, UK.
[6]Department of Chemistry, University of York, York, UK.
[7]School of Environmental Sciences, University of East Anglia, Norwich, UK.

Review Group (*PORG*), 1997]. Studies of ozone production in the free troposphere over Europe, notably at the Jungfraujoch station in the Swiss Alps, have demonstrated that in this region control reverses to be limited by the availability of NO_x [*Zanis et al.*, 2000]. It has been suggested that in situ photochemistry may contribute to the observed ozone spring maximum in the free troposphere [*Penkett and Brice*, 1986; *Monks*, 2000].

[4] Dynamical mechanisms that allow significant quantities of reactive NMHCs to be transported from the boundary layer to the free troposphere will clearly induce substantial deviations from these two established regimes. Although relatively small changes in NMHCs will not directly affect production of ozone ($P(O_3)$) to a large extent, their presence perturbs the distribution of NO_x and reduces the sensitivity of $P(O_3)$ to changes in NO_x. Even if the air is NO_x limited NMHCs will react with, and thus reduce, the concentration of OH and in turn increase the $RO_2:HO_2$ ratio. The extra RO_2 will move the NO_X partitioning towards NO_2 leading to an increase in ozone [*Wayne*, 1996]. NMHCs can also lead to an increase in the production of peroxy acetyl nitrate (PAN) which changes NO_y partitioning allowing NO_x to be transported to remote regions in the form of PAN. Changes in the availability of reactive carbon could have an impact on a number of aspects of radical chemistry, perturbing inorganic to organic peroxy radical partitioning, the OH chemical lifetime and ultimately the tropospheric oxidative capacity.

[5] The atmospheric lifetimes of many reactive NMHCs important in promoting ozone production range between 1 and 15 hours (e.g., $C_2 - C_4$ mono and di-alkenes) and are too short for diffusional mixing to be a significant method of boundary layer - free troposphere exchange. There have been various studies on more rapid vertical redistribution of chemical tracers by convection [*Pickering et al.*, 1988, *Cho et al.*, 1989; *Chatfield and Crutzen*, 1984], but frontal systems have been proposed as a possibly important method for uplift of precursors [*Bethan et al.*, 1998; *Banic et al.*, 1986; *Chaumerliac et al.*, 1992; *Gimson*, 1994; *Fischer et al.*, 2002]. The timescales of such dynamical processes are similar to many alkane and alkene lifetimes, and in this paper we contrast hydrocarbon distributions in the boundary layer and free troposphere under strongly de-coupled conditions and those during frontal activity.

[6] Frontal systems themselves are defined as strong gradients in potential temperature that mark the edges of air masses with different origins and characteristics. Synoptic-scale weather systems often have three major air flows embedded within them which are identified with coherent ascent or descent; warm conveyor belt (WCB); cold conveyor belt (CCB); and dry airstream or intrusion. The dry intrusion is a descending air mass from the upper troposphere or lower stratosphere to the free troposphere and occurs behind the cold front. Both conveyor belt systems consist of an air mass rising from the boundary layer into the free troposphere and have considerable associated convective activity and are therefore capable of uplifting both ozone and precursors. Chemical signatures for stratospheric air in the troposphere such as low CO and NMHCs, high ozone and NO_y are available [*Murphy et al.*, 1993; *Fahey et al.*, 1996], but the 'signature' for uplifted air is not as uniform because emissions and boundary layer concentra-

tions are so variable. During the European Export of Precursors and Ozone by Long-Range Transport (EXPORT) experiment in August 2000, air was sampled under both static conditions and through a cold front passing west to east over central Europe. There we investigated a forward sloping WCB ascending ahead of a kata-cold front as a mechanism for introducing both short and long-lived NMHCs into the free troposphere. A more detailed description of transport in fronts is given by *Browning* [1990].

2. Experimental Details

[7] Whole air samples were collected in 3.2 L silica passivated stainless steel canisters (Thames Restek, UK) pressurized to 2.5 atmospheres using an all stainless steel assembly double headed bellows pump (Metal Bellows, USA), drawing air from the port side forward facing air sample pipe. All transfer lines, unions and gauges were 316 stainless steel in construction. Air samples were analyzed within 48 hours using an automated gas chromatograph with a flame ionization detector, more extensive details of the instrument are given by *Lewis and Bartle* [1996] and *Lewis et al.* [1996]. Automated analysis was achieved using a 16-position autosampler unit to sequentially perform sample, standard and zero measurements. A 1 L aliquot of air was withdrawn from the sample canister and dried using a Nafion permeation device. The hydrocarbons within this gas stream were preconcentrated onto a multibed carbon adsorbent trap held at $-30°C$. Following preconcentration, analytes were transferred at $350°C$ in a stream of helium to an Al_2O_3 porous layer open tubular capillary column (Chrompack, Netherlands) for separation. Peak identification and calibration of NMHC was made by reference to a $1 - 10$ ppbV level 27-component hydrocarbon standard mixture (National Physical Laboratory, Teddington, UK). Detection limits for individual NMHCs ranged between 6 pptV (for propane) and 0.5 pptV (for isoprene) dependent on molecular weight and chemical structure. Signal to noise ratio was found to be 3:1 and both the sample canisters and the standards were reproducible.

[8] Carbon monoxide (CO) was measured by a fast-response fluorescence instrument [*Gerbig et al.*, 1999], with a detection limit of 3 ppbV for a 1 second time interval. The precision of the instrument was ±1.5 ppbV at an atmospheric mixing ratio of 100 ppbV of CO and its accuracy was 5 ppbv + 2.4% for an integration time of 1 second.

[9] A four-channel chemiluminescence analyzer, referred to as the NO_{xy} system, was used to measure nitric oxide (NO), nitrogen dioxide (NO_2) and total reactive nitrogen (NO_y). Here NO_y is defined as $NO_y = NO + NO_2 + HONO + HNO_3 + HO_2NO_2 + NO_3 + 2N_2O_5 + CH_3C(O)O_2NO_2$ (PAN) + other organic nitrates + aerosol nitrate. Detection of NO and NO_2 was achieved by sampling air at 1 L at STP min^{-1} from a rear facing stainless steel tube (to help exclude aerosols >1 μm) lined with 1/4″ (6 mm OD) PFA (perfluoroalkoxy) which was outside the pressure boundary of the aircraft layer and forward of the propellers. NO_2 was converted by photolysis to NO and NO_y species were reduced to NO by CO-catalyzed reduction (0.3% v/v) in gold tubes maintained at $300°C$. The converted sampled air on entering the gold plated reaction vessels was mixed with humidified ozone. Dual NO_y channels allowed the determi-

nation of nitric acid (HNO_3) concentrations since one of the channels (NO_y1) used a denuder (a meter length of $1/4''$ OD nylon tubing) to remove HNO_3 from the sampled matrix. The Teflon inlets used for NO_y measurements were heated to $75°C$ and allowed fast sampling of aerosols up to 4 μm (allowing discrimination of nitrate aerosols) and minimized potential HNO_3 wall losses [*Neuman et al.*, 1999] before the 1 L at STP min^{-1} sampled air reached the heated converter. All overflow and calibration gases entering the NO_y system did so at the inlet. A more detailed description of the instrument is given by *Bauguitte* [2000]. Sensitivity checks of the two NO detectors were determined in-flight by adding a standard concentration of NO in N_2 (Scott speciality gases) of $1.01 ± 0.10$ ppm. The NO standard was diluted into the 1 L STP min^{-1} sample air stream at a rate of 3 cm^3 STP min^{-1} by means of a mass flow controller yielding a resulting mixing ratio of 3.3 ppbV NO. Linear interpolations between the in-flight calibrations were used to provide minimal error. NO_2 calibrations were made possible by photolysis of zero grade air (producing ozone) that reacted with the NO calibration gas to obtain a 90% conversion to NO_2. The conversion efficiency of the NO_2 photolysis cell and gold converters was monitored and did not vary significantly during the flight and was close to 100% for the NO_y converters and 35% for the NO_2 photolysis cell. In flight zeros were performed regularly and zero air artifacts were determined on take-off and landing. The $2σ$ detection limits of the NO_{xy} instrument (based on 10 s averages) were 5 pptV, 9 pptV, 8 pptV and 25 pptV for the NO, NO_2, NO_y and HNO_3 channels respectively.

[10] The back trajectories used in this work were obtained from the ECMWF (European Centre for Medium-Range Weather Forecasts) analyses of the wind using the UGAMP (Universities Global Atmospheric Modelling Programme) offline trajectory model (see *Methven* [1997] and *Methven et al.* [2001] for details). The analyses of vorticity, divergence and surface pressure are transformed to find the 3D velocity in spherical coordinates. The position of each particle is integrated with a time-step (0.25 hrs) that is shorter than the time between wind records (6 hrs). This is achieved by interpolating the winds in space and time to the particle's position and using a 4th order Runge-Kutta integrator method to calculate the path of particles advected by the wind. Fields (e.g., velocity, temperature) at particle positions are obtained by cubic Lagrange interpolation in the vertical followed by bilinear interpolation in the horizontal and linear interpolation in time.

3. Results and Discussion

[11] Data were collected in a series of flights conducted in August 2000 with Deutsches Zentrum für Luft- und Raumfahrt (DLR), near Munich, Germany as the operational base. The C-130 aircraft made 6 flights, each of about 6 hours duration, covering areas over central Europe including: Germany, Austria, Czech Republic, Poland, Slovakia and Hungary. Of these flights four are reported here, which provide information on the distributions of NMHCs over central Europe under conditions of high and low vertical air mass motion.

[12] The flights are summarized as follows: 1. Flights A775 (9/8/00) and A776 (10/8/00) are used to establish

NMHC concentration gradients across a boundary layer/free troposphere interface. 2. Flight A773 (2/8/00) is used to establish the perturbation of vertical distributions in regions of strong convective activity embedded within a frontal system. 3. Flight A774 (3/8/00) is used to establish vertical distributions in the outflow of the warm conveyor belt probed in A773. Altitude, above mean sea level, is calculated from pressure assuming a standard atmosphere.

3.1. Vertical Distribution of Hydrocarbons Under Conditions of Weak Vertical Transport

[13] The vertical gradient in hydrocarbon concentrations in uniform inflow conditions is expected to show a marked decrease at the transition between boundary layer and free troposphere as a result of photochemical removal and limited mixing between these regions. This pattern was confirmed using two flights over central Europe, with a secondary aim of establishing an 'average' boundary layer composition of NMHCs that could be used for source fingerprinting other flights.

[14] The flight tracks for all flights are shown in Figure 1. The boundary layer height was around 2 km throughout the region covered in A775. The boundary layer was turbulent resulting in rapid fluctuations in CO of up to 60 ppb (peaking at 190 ppb) as fresh surface emissions were brought up by eddies. However, potential temperature was well mixed resulting in a neutral profile. A large number of samples were taken during a 200 km long level boundary layer run at 910 m over southern Poland. The average concentrations of NMHCs determined in this boundary layer transect are shown in Table 1. A notable feature was that the variability in many of the hydrocarbon concentrations observed in the bottle samples (taken over 2 minutes) was small, and overall the relative species distribution was very similar for all samples (not shown). Standard deviation in observations was seen to generally increase with atmospheric reactivity in line with many previous studies [e.g., *Jobson et al.*, 1998].

[15] Observations from this flight indicated that the relative mixing ratios of boundary layer hydrocarbons over this region of Europe are not very variable. The average values from this flight have been used subsequently as boundary layer marker distributions when calculating transport timescales based on hydrocarbon reactivity.

[16] Although the flight pattern included several level runs and vertical profiles in the free troposphere there is only limited data with which to compare boundary layer and free troposphere NMHC concentrations. Data was available for CO and NO_x that showed average free tropospheric values of 88 ppbV and 78 pptV respectively, 40 ppbV and 2350 pptV lower than average observations at 910 m height.

[17] Five day 3D back trajectories indicated that the sampled boundary layer air masses had been transported over the Atlantic Ocean at heights of 2–3 km, descending slowly, and were likely to be well processed with respect to NMHCs before entering Europe. Descent into the boundary layer occurred on reaching the continental European land mass and we have therefore considered NMHC content to be from exclusively European emissions.

[18] Flight A776 was performed under very similar meteorological conditions to A775 with greater emphasis on the collection of NMHC samples in both the boundary layer
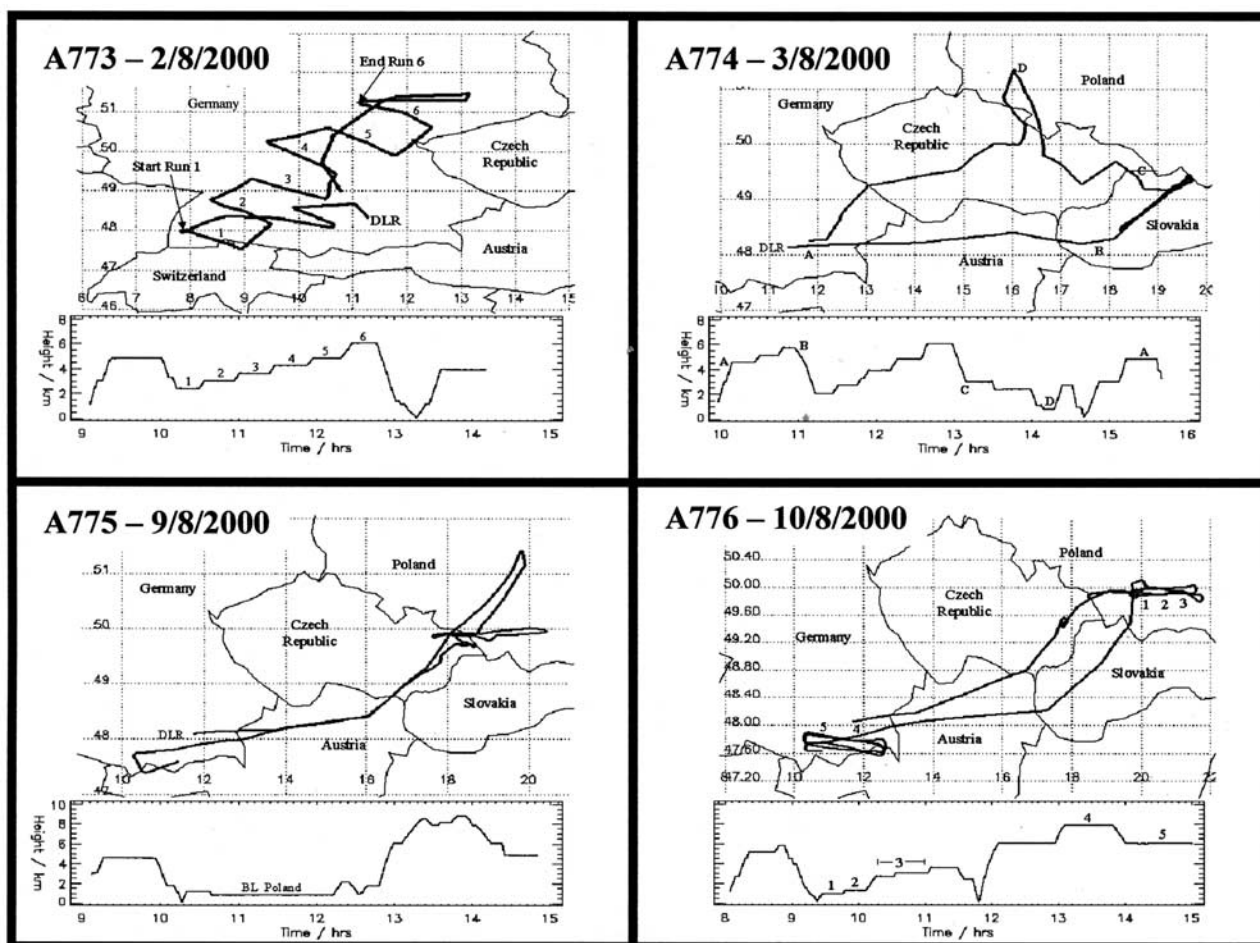
Figure 1. Flight tracks for the four flights investigated.

and free troposphere up to 8 km. Once again potential temperature in the boundary layer was well mixed by strong turbulence but there were rapid fluctuations in CO as fresh surface emissions were brought in by eddies. CO spikes were higher than for A775 (up to 600 ppbV). There were elevated concentrations of both long- and short-lived species, e.g., propane 276 pptV, propene 57 pptV. The ratio of these two compounds remained relatively constant for the level runs (approximately 100 km in length) within the boundary layer (0.20 ± 0.03) indicating emission from common sources. Whole air samples were also collected in the free troposphere over this region and these demonstrate a distinct decoupling between free troposphere and the boundary layer air masses. The vertical distribution of propane and butane are shown in Figure 2.

[19] There was a sharp drop in NMHC mixing ratios towards the top of the boundary layer at 1.8 km, followed by an 800 m thick region of very clean moist air of marine boundary layer origin. Above this, in the free troposphere, NMHC concentrations were found to be relatively constant up to 8 km in height. A thin filament of aged polluted air was observed at 6 km, which trajectory analysis showed to be of North American origin. Averaged data for a selection of species are shown in Table 2, for continental, marine and free tropospheric air. For longer-lived NMHCs such as propane and acetylene, a factor of 3–6 reduction in con-

centration was observed between boundary layer and free troposphere. For shorter-lived NMHCs the differences were, as expected, much more pronounced. For ethene, mixing ratios fell from 100 pptV to below the detection limit of 2 pptV for an increase in altitude from 1.2 to 2.4 km. Similarly many C_4 and C_5 alkanes showed concentrations decreasing by factors of up to 70 over the 1 km covering

Table 1. Average Boundary Layer Concentrations of NMHCs From 14 Samples Collected During Flight A775 at 910 m[a]

	Mixing Ratio (pptV Unless Stated)	Percent Standard Deviation
NO_x, ppbV	2.43	50.2
CO, ppbV	126.28	12.0
Isoprene	22.5	56.7
Propene	41.1	34.2
Ethene	152.9	33.6
N-pentane	92.8	48.9
Iso-pentane	157.2	30.9
N-butane	165.6	50.2
Iso-butane	81.6	43.3
Propane	287.3	22.0
Acetylene	123.3	30.5
Ethane	733.9	13.4

[a]The NMHCs are arranged in order of decreasing reactivity with OH (see Table 3).
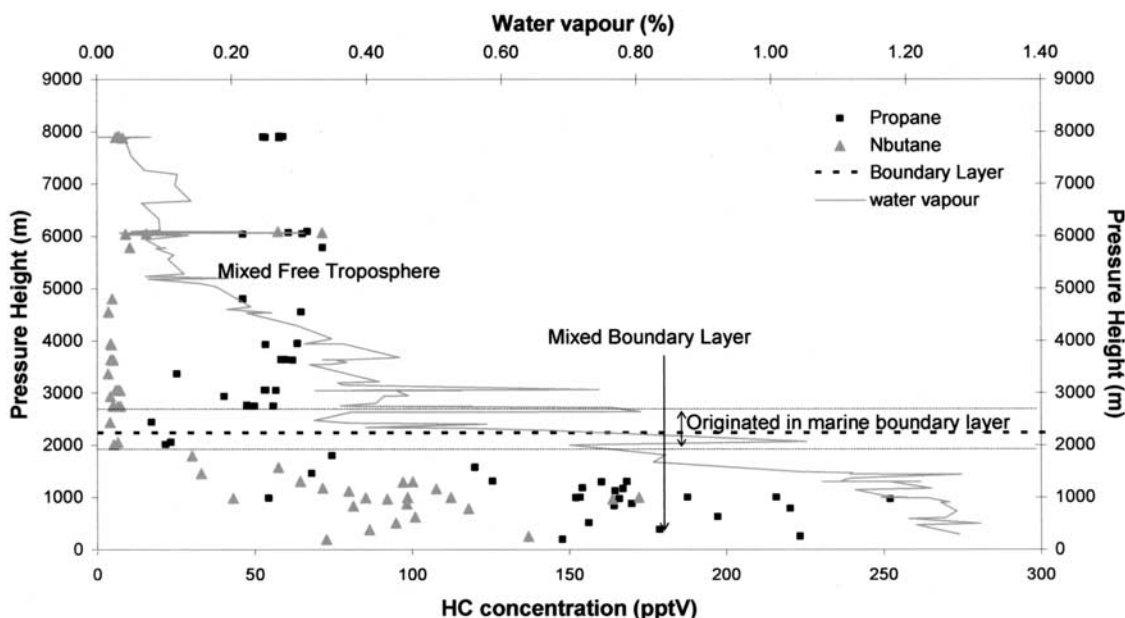
Figure 2. Decoupling between free troposphere and boundary layer using selected NMHC concentrations from A776.

continental boundary layer top to the lowermost free troposphere. The correlation between CO and the long-lived tracer acetylene was high for elements of the flight within the boundary layer (R^2 = 0.76), suggesting a common source region and that both were present as primary pollutants. Correlation between these species for free troposphere sections of the flight was poor suggesting the observed CO in this region may have photochemical origin rather than primary emission. The CO average was taken for the period of the bottle sampling.

[20] Analysis of back trajectories showed that the air masses below 1.8 km had traveled at this altitude for the previous five days, always in the boundary layer, passing over the UK and then continental Europe. Between 1.8 km and 2.6 km air masses had originated in the marine boundary layer and were substantially lower in NMHCs, CO and NO_x compared with both the boundary layer and free tropospheric air masses encountered on this flight. The free troposphere sections of the flight all had air masses that had originally ascended from North America and traveled at around 8 km over the previous three days before descending

over Europe to the height sampled. Whilst the free troposphere NMHC concentrations were substantially lower than the boundary layer observations, comparison with the maritime layer of air encountered on this flight shows that although well processed, it is not equivalent in NMHC terms to maritime 'background' air. Although the concentrations of all fast reacting species had reduced to almost detection limits, the concentration of CO and many alkanes, aromatics and alkynes were substantially higher than the Atlantic boundary layer background. In this respect a measurable degree of intercontinental transport of organic pollution to Europe was seen to be occurring. Typical boundary layer and free troposphere trajectories for A776 are shown in Figure 3.

3.2. Uplift of Reactive NMHCs in a Cold Frontal System

[21] The essentially decoupled nature of the boundary layer and free troposphere under the conditions encountered in flights A775 and A776 resulted in NMHC abundances that would play only a very minor role in free tropospheric

Table 2. Average Concentrations Under Decoupled Boundary Layer-Free Troposphere Conditions During Flight A776

|	Run 1: 1.1 km (Boundary Layer - BL)	Run 2: 1.4 km (BL)	Run 3: 2–3 km (Originated Marine BL)	Run 4: 7.9 km (Free Troposphere)	Run 5: 6.1 km (Free Troposphere)
CO, ppbV	133.57 ± 90.37	145.3 ± 87.59	64.25 ± 2.60	66.85 ± 2.71	76.93 ± 8.54
Propene, pptV	35.5 ± 26.8	43.2 ± 18.8	26.7 ± 14.4	10.2 ± 3.1	15.0 ± 8.2
Ethene, pptV	102.6± 41.3	145.3 ± 66.8	30.3 ± 18.8	BDL[a]	21.0 ± 8.2
N pentane, pptV	60.6 ± 30.7	58.4 ± 14.0	6.9 ± 1.6	8.3 ± 2.2	8.7 ± 2.7
Isopentane, pptV	95.4 ± 27.7	77.4 ± 14.1	4.6 ± 1.3	2.6 ± 0.8	7.1 ± 0.9
N butane, pptV	85.5 ± 19.1	92.3 ± 19.1	5.3 ± 1.2	7.0 ± 0.9	9.2 ± 5.9
Isobutane, pptV	43.0 ± 16.3	49.4 ± 9.0	3.6 ± 1.3	3.9 ± 0.4	6.1 ± 2.1
Propane, pptV	135.0 ± 57.1	155.3 ± 20.1	21.0 ± 3.1	56.3 ± 2.9	65.4 ± 27.1
Acetylene, pptV	96.8 ± 29.6	89.6 ± 25.1	10.5 ± 3.6	15.8 ± 2.2	17.7± 6.9
Ethane, pptV	617.7 ± 64.3	604.1 ± 74.3	355.6 ± 30.0	420.7 ± 30.0	487.9 ± 87.7

[a]BDL = below detection limit.
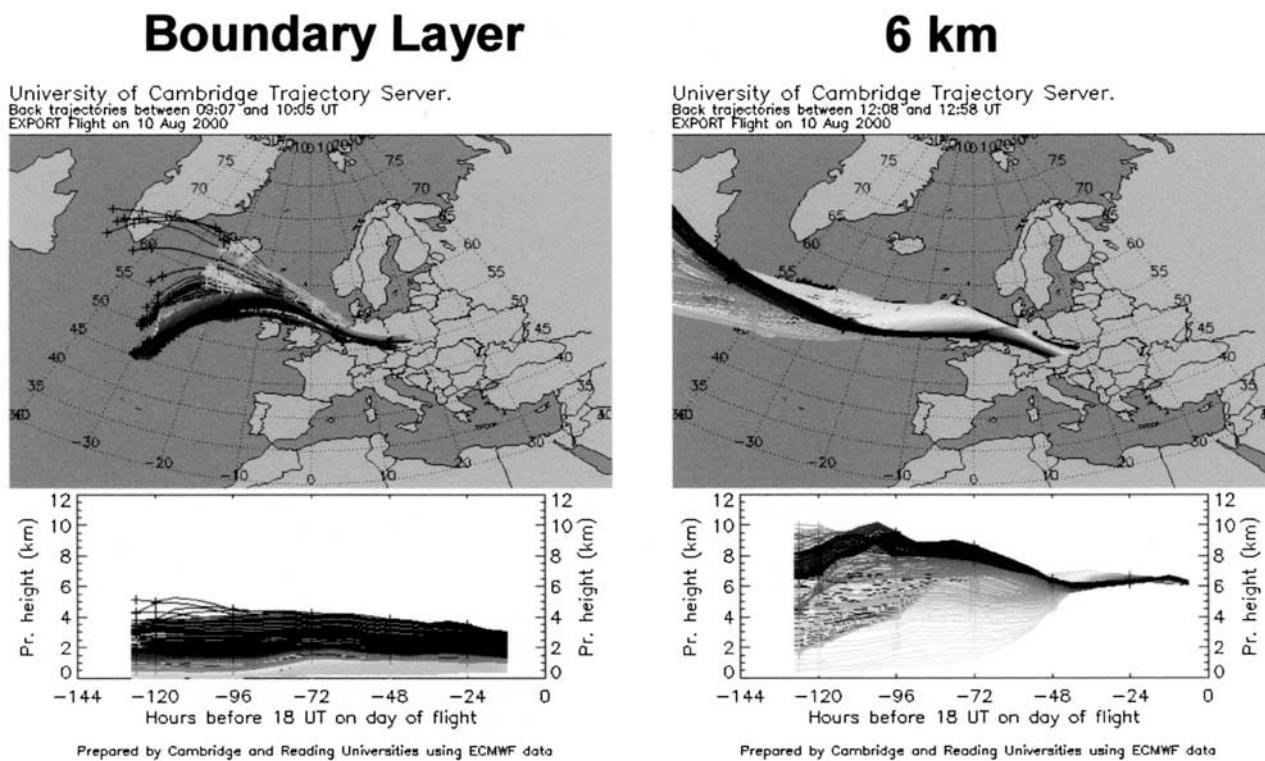
Figure 3. Three-dimensional back-trajectories for flight A776.

ozone chemistry. Even when long-range transport of pollution was observed, such as in the free troposphere in flight A776, the vast majority of reactive NMHCs had been oxidized. When hydrocarbons are viewed purely as routes for OH loss (for example excluding radical regeneration *via* oxygenated intermediate photolysis), they account for less than 7% of the free troposphere OH sink budget, calculated from reaction rates, methane, CO, NO_2 and hydrocarbon measurements.

[22] For in situ ozone production to be substantially perturbed by NMHCs from the boundary layer there must be rapid ventilation of recently polluted boundary layer air into the free troposphere. Uplift of fresh boundary layer air was encountered in flight A773 (2/8/00) *via* a cold front, its associated warm conveyor belt (WCB) and convective activity. Whilst frontal systems have been previously recognized as important mechanisms in the vertical distribution of pollutants [*Bethan et al.*, 1998; *Banic et al.*, 1986; *Chaumerliac et al.*, 1992; *Gimson*, 1994] measurements have generally focused on conserved or long lived tracers, and reports of uplift of NMHCs are very limited. A major feature of the front is the WCB and its upward flow of air along and ahead of the advancing cold front. Warm air is drawn into the cloud belt from the convective boundary layer at low altitudes and rises into the free troposphere as it travels within the cloud belt.

[23] Conveyor belts were first described by *Harrold* [1973] based on the analysis of system relative flow along layers of constant wet bulb potential temperature using radiosonde data. Radar observations were used to locate precipitation patterns relative to the weather systems. K. Browning and collaborators have used this analysis technique and more recently satellite observations of cloud

patterns to construct conceptual models for frontal system development within synoptic-scale weather systems (see review given by *Browning* [1990]).

[24] The synoptic situation at the time of flight A773 can be assessed from the Meteosat IR channel image (Figure 4a). A band of cloud stretches from the Pyrenees to the Baltic. The highest cloud (lowest brightness temperature) forms an arc across Northern Germany. The band of cloud is associated with a WCB running parallel to and ahead of a weak surface cold front. The leading edge of ascending air near the north coast of Germany is referred to as the head of the WCB. The parent low is mature and can be seen centered over Northern Ireland. One day later (Figure 4b) the foot of the WCB is still over Spain and the cloud band extends over southern Germany around the west side of the Alps. However, further north of the Alps the front has run eastwards and the air that was in the head of the WCB on August 2 has reached the extreme northeast corner of the domain in Figure 4b.

[25] The vertical structure of the frontal system is revealed using reverse domain filling trajectories for a 3D grid (RDF3D). Three day back trajectories were calculated from a regular grid covering the domain shown by a box in Figure 4a on levels ranging from the ground to 11 km (spacing 0.4 degrees in longitude, 0.25 degrees in latitude and 0.25 km in altitude). In Figure 5 the value of pressure from the origin of each trajectory is used to color its arrival point on the grid. Red shading indicates air that was below 850 hPa three days beforehand. Figures 5a and 5b show the results for the 724 hPa and 616 hPa levels of the grid. Both show how the trajectories arriving along the arc of the WCB have originated from the boundary layer. Panel 5c shows the vertical cross-section XY through the domain, roughly

IR Meteosat Satellite Data 2/8/00 12Z

a

IR Meteosat Satellite Data 3/8/00 12Z

b
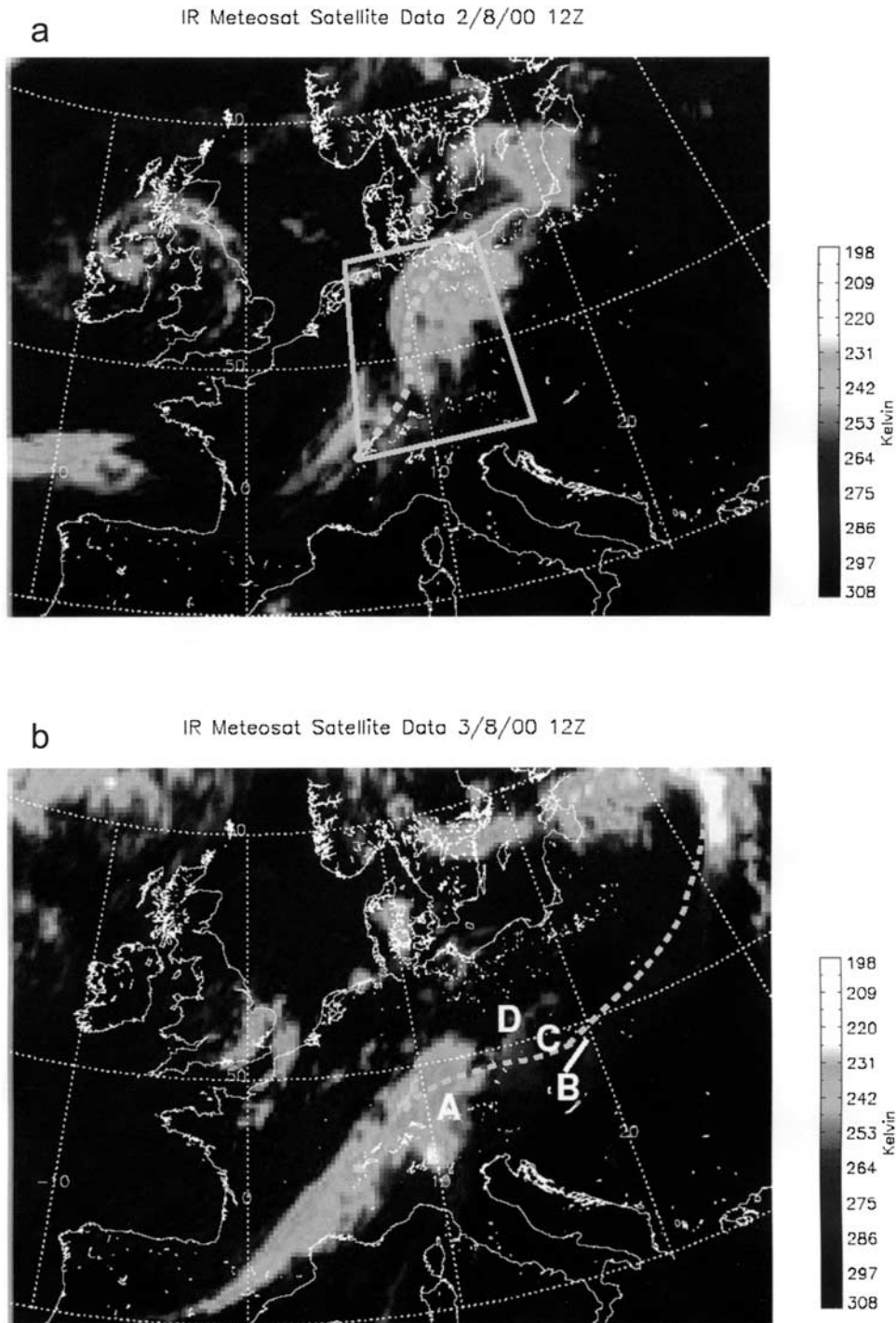
Figure 4. Meteosat IR channel brightness temperature at 12 UT on (a) 2 August and (b) 3 August 2000. The dashed lines mark the northwest edge of the warm conveyor belt as determined from RDF3D trajectories (see text). Flight A773 was centered around 50N, 10E on August 2 and the box marks the RDF3D domain shown in Figure 5. On August 3, letters A–D mark positions along flight A774 (see Figure 1) and the white line marks the ascending stack of five levels over Slovakia (between 11:00 and 13:00 UT).

along the axis of the WCB. It is clear how the WCB slopes up towards point Y and the head has reached 4 to 5 km. The air originating from the boundary layer (red color) lies further to the east at 616 hPa than at lower levels (724 hPa) at all latitudes, indicating that the WCB is forward sloping associated with a kata-cold front. Figure 6 shows equivalent potential temperature, EPT, on section AB across the frontal system. There is a clear maximum sloping forward from the surface front (near 150 km along AB) to 600 hPa (around 550 km along AB). Note that the fine-scale
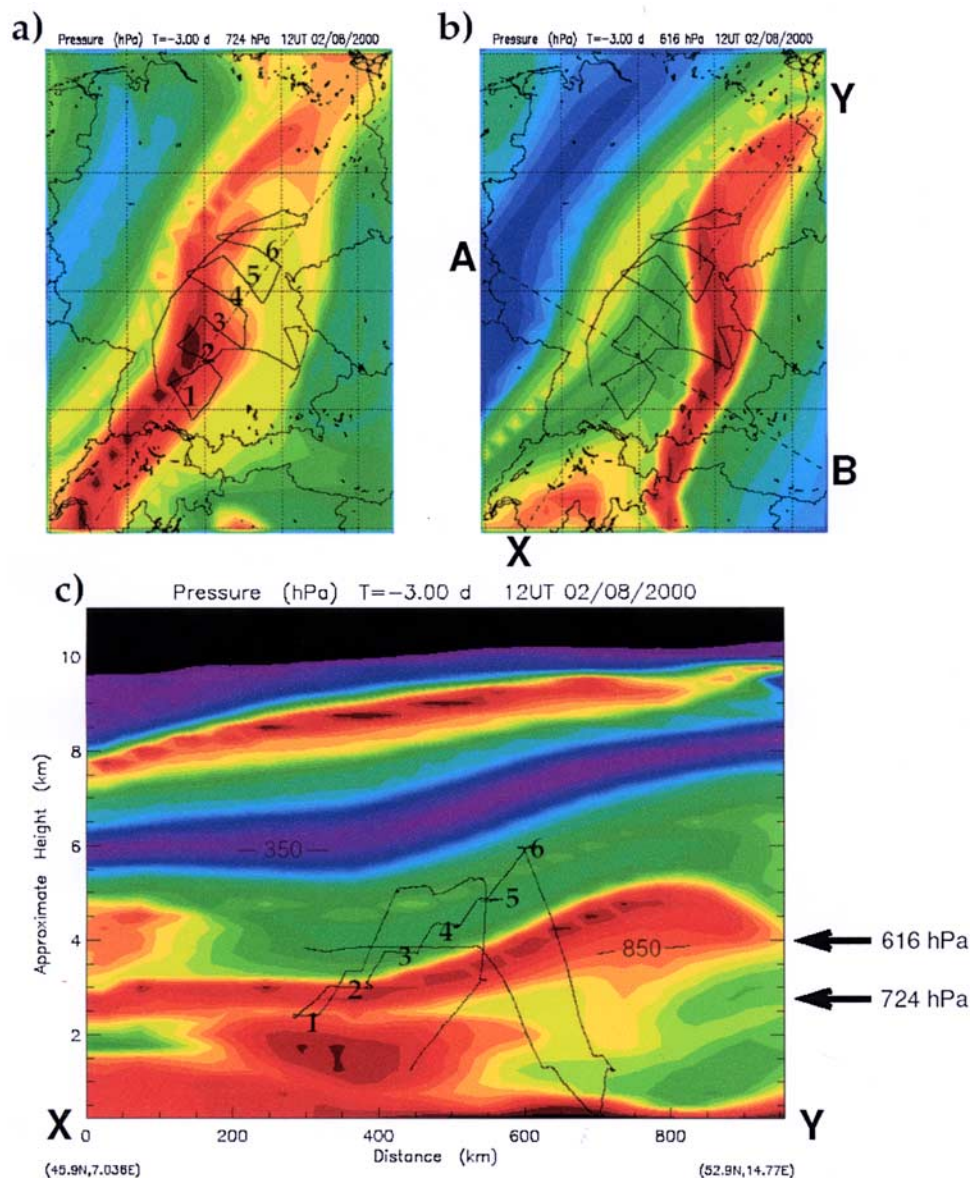
Figure 5. Structure of the warm conveyor belt at 12 UT August 2000 as seen by RDF3D analysis. Three-day back trajectories are calculated from a 3D grid and each grid point is colored by the pressure at the origin of the corresponding trajectory (p > 850 hPa red; p < 350 hPa indigo; CI = 25 hPa). Red denotes air that can be traced back to the boundary layer following the resolved winds. (a) Trajectories arriving at 724 hPa, (b) trajectories arriving at 616 hPa and (c) cross section XY through the 3D arrival grid. The flight track is shown relative to the air at 12 UT and legs 1–6 are labeled.

structure shown in EPT was simulated by using RDF3D trajectories and assigning to each grid point the EPT interpolated from ECMWF analyses to the origin of the trajectory. EPT was taken from half way along the 3 day trajectories and is similar to the average value along each trajectory. Note that the ECMWF analyses at the single time frame (12 UT 2/8/2000) do not have sufficient resolution to pick out the sloping maximum in EPT. The front slopes further forward to the south of the domain, but is still forward sloping near point Y.

[26] This case fits very well with the conceptual model of a forward sloping WCB shown in Figures 5a and 9 of *Browning and Monk* [1982] and the associated cloud

pattern. The dashed curve in Figure 4a follows the northwest edge of the boundary layer air that has reached 700 hPa (red band in Figure 5a). It is clear that the mesoscale structure seen in the RDF3D simulation lies along the same curved shape as the observed cloud band. Notably, the highest cloud lies just to the northwest of the curve. Since the curve passes through the section AB at a distance of approximately 300 km along AB, the front-relative location of the high cloud is about 250 km along AB. It is plausible that the high cloud is a band of ''upper cold frontal convection'' characteristic of the forward sloping ascent, split front situation depicted by *Browning and Monk* [1982]. In this situation the deepest convection is expected along the
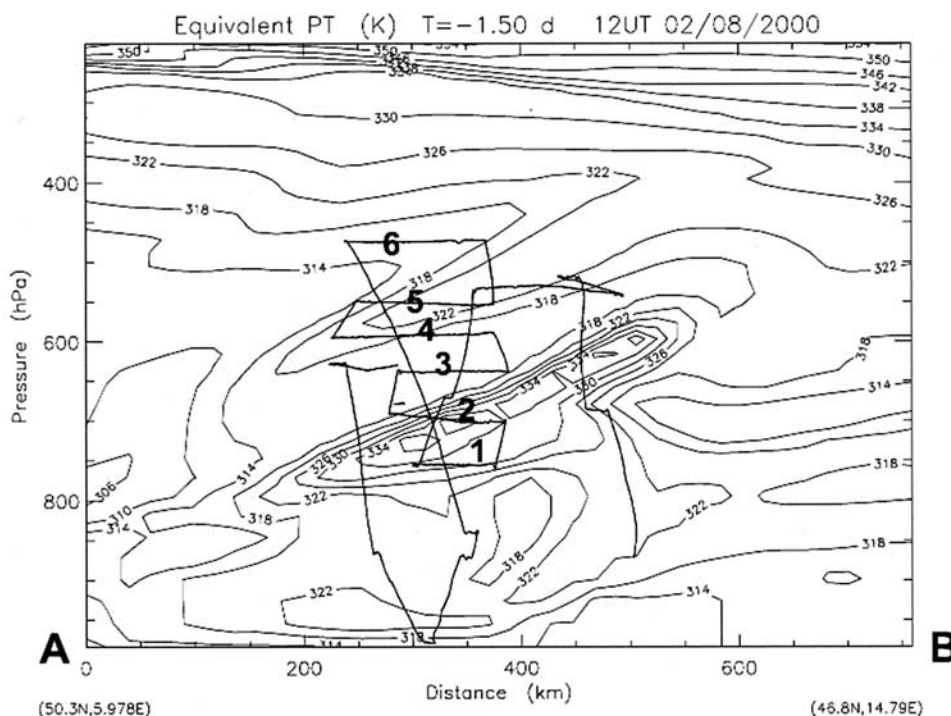
Figure 6. Equivalent potential temperature (EPT) on section AB across the frontal system (see Figure 4b).

line of the upper cold front and mid-level convection lies ahead embedded in the WCB.

[27] The flight track of the C-130 aircraft is shown on Figures 5 and 6. It is shown relative to the air masses at the reference time 12 UT by following air mass trajectories from points spaced at 10 s intervals along the track backwards or forwards to 12 UT. The figures indicate that the aircraft flew directly through the WCB on runs one and two. Back trajectories from run two (see Figure 7), calculated following the flow resolved by the ECMWF analyses, can be traced back to the boundary layer near the Pyrenees two days beforehand. Note that back trajectories from runs 3−5 also indicate ascent within the frontal system over the last two days but they originated above the boundary layer. Back trajectories from run 6 originate much further west and descend before frontal ascent during the last 30 hours.
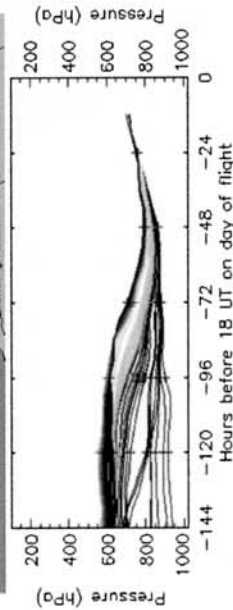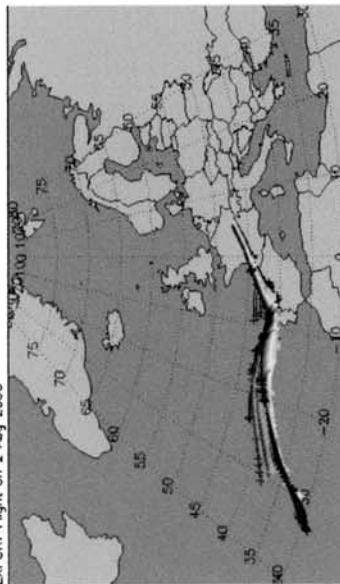
[28] Note that if vertical transport only occurred following the analyzed flow (necessarily on scales of 50 km or greater, given the observing network and the forecast model) then we would expect only runs one and two to be polluted air. The time elapsed for the resolved scale ascent (1.5 days) is sufficient for the majority of fast reacting species to be oxidized and processed before interception by the aircraft. However, convection is always embedded within a WCB, as inferred from the satellite image, and results in unresolved (subgrid-scale) transport in convective updrafts and the compensating subsidence. If the cloud base for this convection is low enough, convective updrafts could bring pollutants to the level of the aircraft in an hour before short-lived hydrocarbons have been oxidized. Thus the relative roles in transport for large-scale ascent along the frontal surface and convective updrafts are important to the distribution of hydrocarbons and the photochemical activity of the free troposphere.

[29] Figure 8 shows the variation in concentrations of selected hydrocarbons, CO and some NO_{xy} species at differing altitudes. NMHC concentrations increased significantly in the center of some level runs (marked 1−6) in the regions of strong convective activity preceding the surface front. The large differences in for example alkene concentrations exposed these transitions between convective and nonconvective regions more clearly than longer-lived tracers such as CO, which have been used previously. The NMHC mixing ratios are correlated to the profile of convective influence within the WCB, which showed a maximum on Run 2, decreasing to Run 4 and with no influence at the altitude of Run 5. The mixing ratios increase once more on Run 6, possibly because the end of the run was close to the upper frontal convection shown on the satellite image. The vertical wind component detected by the aircraft is also shown on Figure 8a. The flight legs experiencing large vertical velocity in short bursts were also those where CO, NMHCs and NO_y show strong spikes in concentration, indicating the influence of convective updrafts. Note that the concentration spike in all compounds coincides with the largest spike in vertical velocity (10:41 UT) of about 2.5 m/s, suggesting that the aircraft flew through a convective updraft from the polluted boundary layer below.

[30] The high proportions of alkenes relative to alkanes observed in regions of front indicate that the timescale for their uplift from the boundary layer to the free troposphere is of the order of hours rather than days. To establish this timescale more precisely and to confirm that associated and embedded convection dominates over advective slantwise ascent within the WCB, the ratios of individual reactive hydrocarbons to the relatively long-lived NMHC tracer acetylene were calculated. Comparing NMHC ratios eliminates the effects of dilution and allows an analysis of
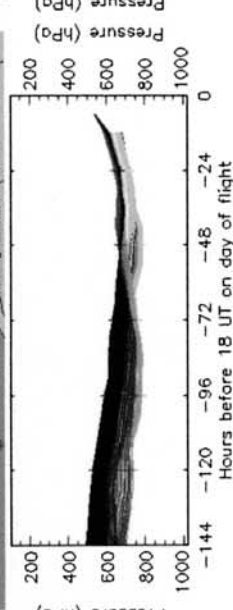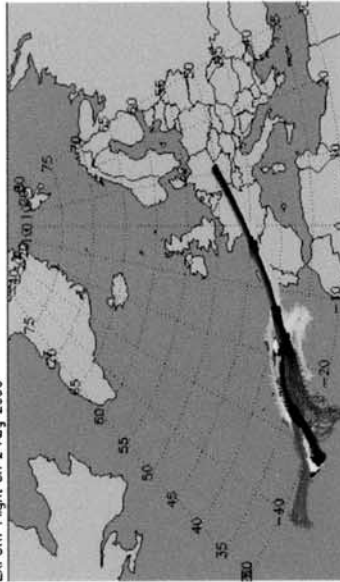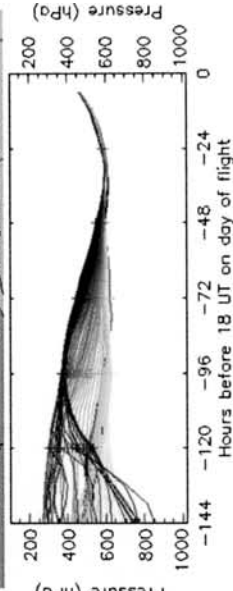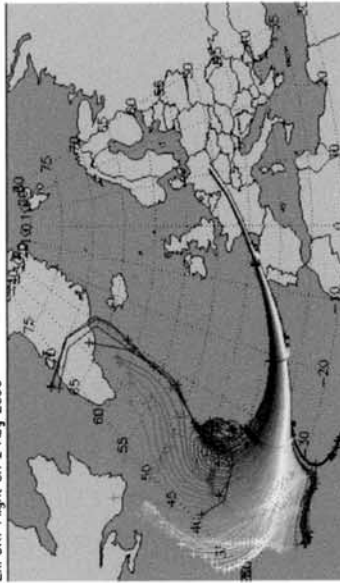
Figure 7. Trajectory results from Runs 2–6 for flight A773.
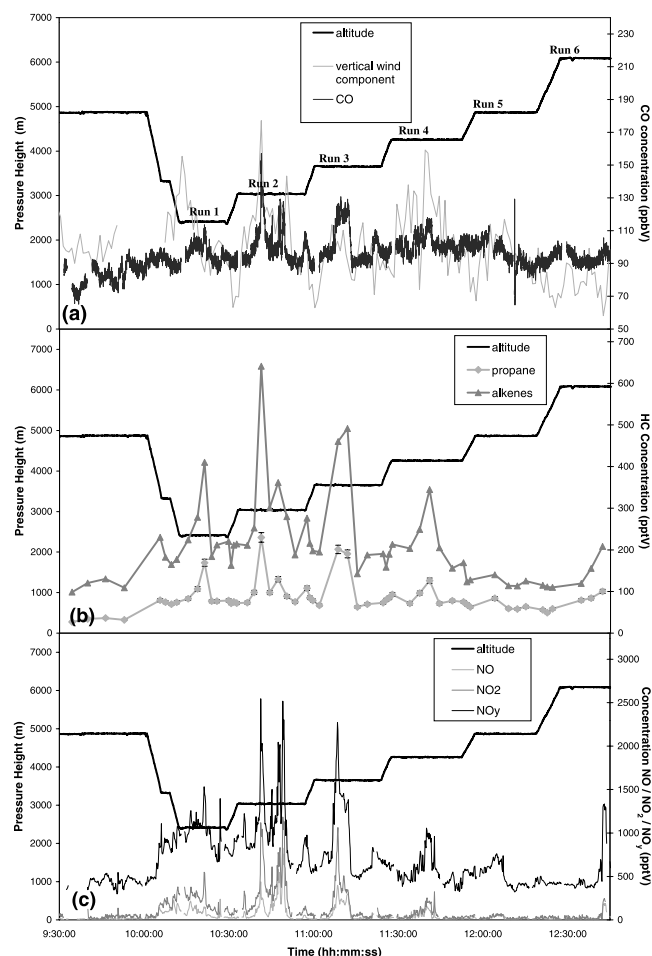
Figure 8. Time series for A773 showing (a) CO and vertical velocity in ms^{-1} (10 second average, offset by +3 and scaled by 40) (b) Propane and alkenes (c) NO, NO$_2$, NO$_y$.

transportation time based upon differing reactivities with OH, i.e. a "chemical clock" - a decreasing ratio of short-lived hydrocarbon to long-lived hydrocarbon indicating an increasingly aged air mass. Calculations of this sort make a number of important assumptions, firstly the source in the

boundary layer is homogeneous, and secondly that dilution is by air of zero concentration.

[31] Table 3 shows the ratios of a number of NMHCs with respect to acetylene. For propene and ethene at the center of Run 1 at 2.4 km their ratios were very similar to those obtained within the boundary layer in flights A775 and A776. As runs were conducted crossing the front at increasing altitude, the ratios of most NMHC species to acetylene remained constant up to an altitude of 4.3 km, implying rapid uplift from the boundary layer to the free troposphere. To estimate the timescale for uplift the most abundant reactive species isoprene was used, since its atmospheric 1/e lifetime under typical $1-3 \times 10^6$ molecules cm^{-3} of OH conditions, is only $1-2$ hours. The observations showed that at 4.3 km there had been no statistically significant reduction in its ratio relative to acetylene, in turn suggesting that this uplift from surface level must be occurring over periods of less than 1 or 2 hours. Using 2 hours as an upper limit for the transport timescale, this equates to a vertical velocity of 0.6 ms^{-1}. This is comparable to the measured vertical wind speed from the aircraft data, which gave an average of 0.5 ms^{-1} for the runs within the WCB. These observations of constant 'boundary layer' like alkene/acetylene ratios are considered possible only by convective activity caused by the WCB rather than the large-scale advection which had occurred over a period of several days previously (compare Figure 7). Whilst for Run 1 and 2 there is a sharp increase in NMHCs in the center of each level run due to convective uplift, for longer-lived tracers such as NO$_y$, the feature is much broader, extending right across the run. This indicates that WCB advection *is* bringing substantial boundary layer pollution into the free troposphere but that it is depleted in reactive carbon content. In Runs $3-4$ NO$_{xy}$ concentrations follow much more closely those of the NMHCs. In these cases it appears that convective activity alone is driving the composition. Trajectory analysis supports this, indicating that WCB ascent at these levels began above the boundary layer.

[32] The front observed in A773 was a relatively weak cold front and therefore high-altitude convection was not associated with the system. From measurements of cloud top height the convection in this case appeared to be reaching levels of approximately 4 km, a figure in agreement with the NMHC, CO and NO$_{xy}$ observations. At 4.9 km

Table 3. NMHC Ratios With Respect to Acetylene at Different Altitudes in the WCB and in the Boundary Layer

	K$_{OH}$ $\times$ 10^{13}, [a] cm^3 molecules^{-1} s^{-1}	1/e Lifetime,[b] hours	Run 1: 2430 m	Run 2: 3050 m	Run 3: 3660 m	Run 4: 4270 m	Run 5: 4880 m	Run 6: 6100 m
CO, ppbV	1.3	1335.42	110.21 ± 6.28	109.43 ± 16.81	110.90 ± 17.32	106.15 ± 6.21	94.94 ± 4.43	Present
Acetylene, pptV	8.15	170.42	37.7 ± 10.0	57.5 ± 27.6	48.6 ± 19.4	31.4 ± 1.8	44.1 ± 5.3	Present
Isoprene/C$_2$H$_2$ ratio	1010	1.38	0.18	0.28	0.19	0.15	<0.03	Present
1,3 butadiene/C$_2$H$_2$ ratio	666	2.09	0.53	0.56	0.60	0.57	<0.03	Present
Propene/C$_2$H$_2$ ratio	263	5.28	0.58	0.57	0.43	0.45	0.36	Present
Ethene/C$_2$H$_2$ ratio	85.2	16.30	1.24	1.21	1.54	0.78	<0.18	Present
N pentane/C$_2$H$_2$ ratio	39.6	35.07	0.85	0.70	0.80	0.60	0.40	Present
Iso pentane/C$_2$H$_2$ ratio	39.0	35.61	2.20	1.84	2.20	1.41	0.49	Present
N butane/C$_2$H$_2$ ratio	25.4	54.68	1.40	1.33	1.77	1.34	0.63	Present
Iso butane/C$_2$H$_2$ ratio	23.3	59.61	0.85	0.81	0.97	0.78	0.35	Present
Propane/C$_2$H$_2$ ratio	11.5	120.77	3.45	2.60	3.26	2.62	2.56	Present
Ethane/C$_2$H$_2$ ratio	2.5	540.42	10.20	10.7	9.2	10.05	13.82	Present

[a]*Atkinson* [1997].
[b]OH concentration = 2×10^6 molecules cm^{-3}.
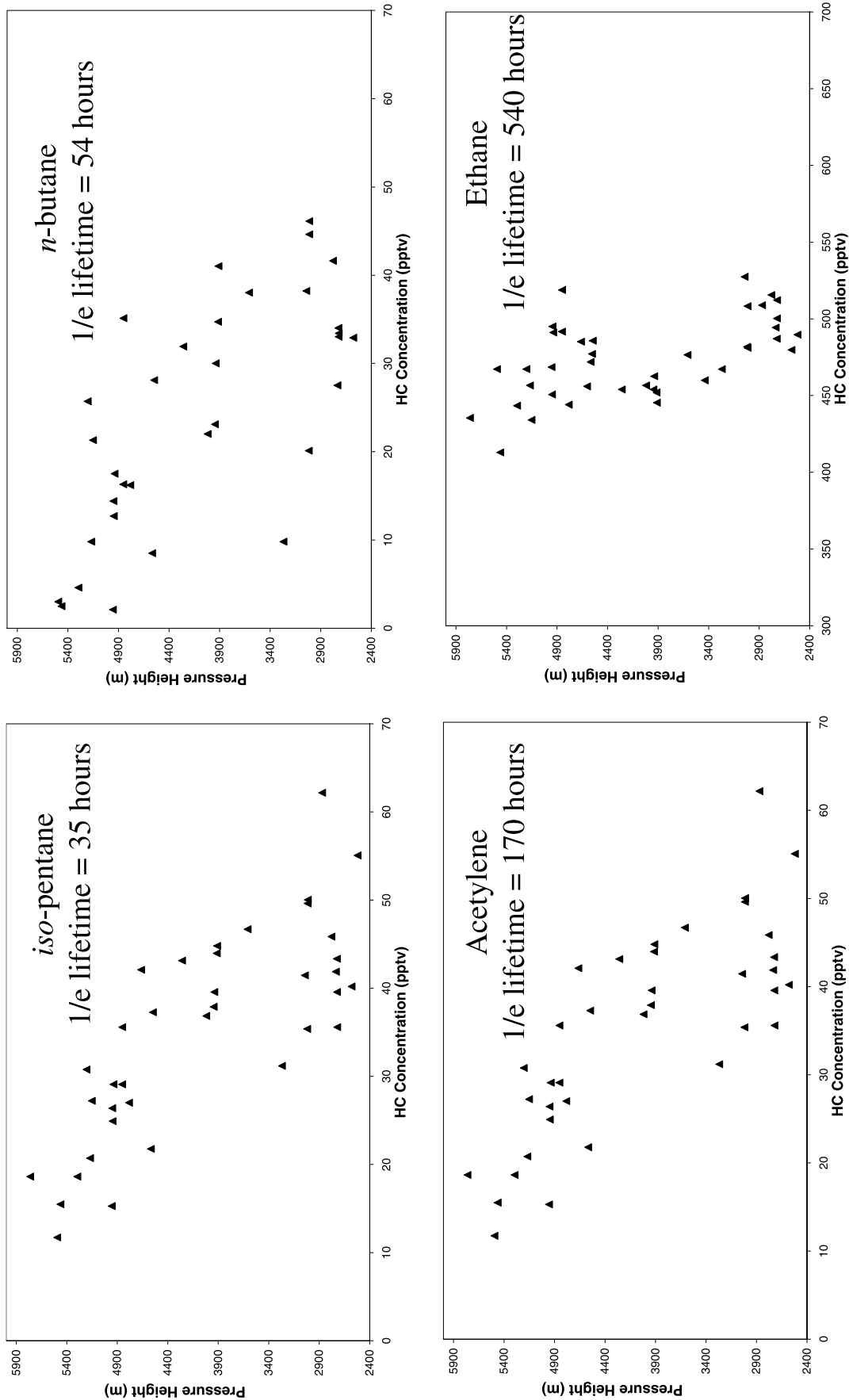
Figure 9. Vertical profiles of four NMHCs with different timescales (hrs) for reaction with OH (shown by the numbers in each panel) in the free troposphere during flight A774.

on Run 5 the ratios of reactive to unreactive species decreased significantly in line with this level being above the influence of associated convection. There was however a slight increase in mixing ratio for all NO_{xy} species in the center of the level run, suggesting that some weak slow moving vertical motion due to the WCB had occurred. The highest altitude crossing of this region in Run 6 does not appear to be in air directly affected by the frontal system itself, although levels of all species were seen to increase at the far Western edge of the level run. This increase in mixing ratios may be due to deep upper cold frontal convection (see Figure 8.10 of *Browning* [1990]) located above the surface front. The actual hydrocarbon values are not shown in Table 3 for Run 6 as there is very limited data coverage however all species were observed above detection limits at this altitude.

[33] Flight A774 (3/8/00) took place the day after the frontal system had been sampled in A773. On 3 August 2000 the main slantwise ascent and convection associated with the WCB still lies to the southwest of Munich (point A in Figure 4b) and the aircraft sampled air to the east that had been uplifted 12–24 hours previously within the WCB system. The C-130 aircraft flew on 5 stacked levels over Slovakia in mainly clear air outflowing horizontally from the WCB (along bold, white line marked on Figure 4b and also Figure 1). Although no longer convectively active the WCB outflow can be traced (using RDF3D analysis-not shown) along the dashed line to the deep convection that had been part of the WCB head on 2 August (northeast corner of Figure 4b).

[34] The vertical profiles obtained on this flight for a number of NMHCs are shown in Figure 9. In general, concentrations of long and medium lived hydrocarbons were seen to be substantially elevated above the free tropospheric levels seen during flights A775 and A776 when air mass vertical motion was limited. Concentrations of reactive species such as alkenes were however significantly lower than those observed on A773. Analysis of back trajectories for this flight indicated that for the vast majority of samples collected, air masses were of Atlantic origin ascending over Europe during the previous 1–2 days as part of the WCB system ahead of the cold front. Despite encountering some broken cloud and shallow convection, reactive species were at very much lower levels than seen in the flight that crossed the WCB itself. As in A773, above 5 km air mass trajectories were predicted to be above the effects of the front remaining at high altitude for 5 days previously. This was supported by chemical measurements, which showed sharp decreases in concentration above this altitude.

4. Conclusions

[35] During periods of limited vertical air mass motion (A775 and A776) the vertical distribution of NMHCs in the boundary layer and free troposphere were determined over central Europe. Free tropospheric concentrations for longer lived alkanes were between 3 to 6 times lower than average boundary layer values, whilst for short lived species the difference was more pronounced, differing by up to a factor of 100. Air masses of North American boundary layer origin arriving at high altitude over central Europe were seen to have elevated levels of many longer-lived hydrocarbons when compared to air masses of oceanic boundary layer origin. Whilst intercontinental transport of certain hydrocarbons was observed, the reactivity of the hydrocarbons in the air mass was low and likely to play only a small role in influencing ozone photochemistry.

[36] In contrast to the weak vertical transport conditions of A775 and A776, flight A773 sampled air in the warm conveyor belt region present ahead of the cold front and A774 sampled air previously uplifted within the WCB system. However, reactive species were seen at much lower concentrations in flight A774 than observed in the flight crossing the active WCB the day before. On both days, back trajectories from flight levels above 4.5 km do not show any ascent over the last 5 days and remain above the effects of the frontal system. In regions of the front enhanced concentrations of both long and short-lived hydrocarbons were observed along with other pollutants such as NO_x and CO. The timescale of ventilation from the boundary layer, and hence the vertical velocity of this process, was examined using NMHC ratios as a multiple tracer. The presence of boundary layer like ratios of alkenes to acetylene indicated that embedded and associated convection rapidly transported the highest observed concentrations of NMHCs, rather than air masses which had undergone slower, slantwise ascent along the WCB following the winds resolved in atmospheric analyses. In many regions of the WCB system, the time period for transport was too fast for any statistically significant change in alkene to acetylene ratios to be observed, however a lower limit of estimated vertical velocity of 0.6 ms^{-1} has been made which is comparable to the 0.5 ms^{-1} vertical wind speed taken from aircraft data. Whilst it was not possible to assess the relative amounts of reactive carbon introduced by the two transport mechanisms, correct parameterization of the convection in the front will be important if free tropospheric ozone creation is to be correctly modeled.

[37] Five air masses were observed where the difference in composition can be explained approximately by the time since last encountering sources and the NMHC reactivity with OH. In decreasing order of NMHC concentration they were: the polluted continental boundary layer, an active WCB as part of a cold frontal system, the horizontal outflow 12 hours downstream from the same WCB, a mid-tropospheric air mass from North America and air coming directly from the marine boundary layer. The time since encountering fresh emissions is respectively: <10 minutes, <2 hours, <24 hours, <4 days and 5 days. Although there was only relatively weak ascent within the WCB sampled during this experiment, this is typical of conditions encountered in Europe during summer time (when photochemistry is also most active). The relative extent to which slantwise ascent and embedded convection within a WCB system may influence free tropospheric chemistry is a key question that should be addressed through further modeling and more case studies.

References

Atkinson, R., Gas-phase tropospheric chemistry of volatile organic compounds, 1, Alkanes and alkenes, *J. Phys. Chem. Ref. Data*, *26*, 215–290, 1997.

Banic, C. M., G. A. Isaac, H. R. Cho, and J. V. Iribane, The distribution of pollutants near a frontal surface: A comparison between field experiment and modelling, *Water Air Soil Pollut.*, *30*, 171–177, 1986.

Bauguitte, S. J. B., A study of tropospheric reactive nitrogen oxides in the North Atlantic region, Ph.D. thesis, Univ. of East Anglia, Norwich, England, 2000.

Bethan, S., G. Vaughan, C. Gerbig, A. Volz-Thomas, H. Richer, and D. A. Tidderman, Chemical air mass differences near fronts, *J. Geophys. Res.*, *103*, 13,413–13,434, 1998.

Browning, K. A., Organization of clouds and precipitation in extratropical cyclones, in *Extratropical Cyclones*, pp. 129–153, Am. Meteorol. Soc., Boston, Mass., 1990.

Browning, K. A., and G. A. Monk, A simple model for the synoptic analysis of cold fronts, *Q. J. R. Meteorol. Soc.*, *108*, 435–452, 1982.

Carpenter, L. J., T. Green, G. Mills, S. A. Penkett, P. Zanis, E. Schuepbach, and P. S. Monks, Oxidised nitrogen and ozone production efficiencies in the springtime free troposphere of the Alps, *J. Geophys. Res.*, *105*, 14,547–14,559, 2000.

Chatfield, R. B., and P. J. Crutzen, Sulphur dioxide in remote oceanic air: Cloud transport of reactive precursors, *J. Geophys. Res.*, *89*, 7111–7132, 1984.

Chaumerliac, N., R. Rosset, M. Renard, and E. C. Nickerson, The transport and redistribution of atmospheric gases in regions of frontal rain, *J. Atmos. Chem.*, *14*, 43–51, 1992.

Cho, H. R., M. Niewiadomski, J. V. Iribarne, and O. Melo, A model of the effect of cumulus clouds on the redistribution and transformation of pollutants, *J. Geophys. Res.*, *94*, 12,895–12,910, 1989.

Fahey, D. W., S. G. Donnelly, E. R. Keim, R. S. Gao, R. C. Wamsley, L. A. Del Negro, E. L. Woodbridge, M. H. Proffitt, and K. H. Rosenlof, In situ observations of NO_y, O_3 and the NO_y/O_3 ratio in the lower stratosphere, *Geophys. Res. Lett.*, *23*, 1653–1656, 1996.

Fischer, H., et al., Synoptic tracer gradients in the upper troposphere over central Canada during the Stratosphere-Troposphere Experiments by Aircraft Measurements 1998 summer campaign, *J. Geophys. Res.*, *107*(D8), 4064, doi:10.1029/2000JD000312, 2002.

Gerbig, C., S. Schmitgen, D. Kley, A. Volz-Thomas, K. Dewey, and D. Haaks, An improved fast response vacuum UV resonance fluorescence CO instrument, *J. Geophys. Res.*, *104*, 1699–1704, 1999.

Gimson, N. R., Dispersion and removal of pollutants during the passage of an atmospheric frontal system, *Q. J. R. Meteorol. Soc.*, *120*, 139–160, 1994.

Harrold, T. W., Mechanisms influencing the distribution of precipitation within baroclinic disturbances, *Q. J. R. Meteorol. Soc.*, *99*, 232–251, 1973.

Holton, J. R., P. H. Haynes, M. E. McIntyre, A. R. Douglass, R. B. Rood, and L. Pfister, Stratosphere-troposphere exchange, *Rev. Geophys.*, *33*(4), 403–439, 1995.

Intergovernmental Panel on Climate Change (IPCC), Aviation and the global atmosphere, special report, Geneva, 1999.

Jobson, B. T., D. D. Parrish, P. Goldan, W. Kuster, F. C. Fehsenfeld, D. R. Blake, N. J. Blake, and H. Niki, Spatial and temporal variability of nonmethane hydrocarbon mixing ratios and their relation to photochemical lifetime, *J. Geophys. Res.*, *103*, 13,557–13,567, 1998.

Lacis, A. A., D. J. Wuebbles, and J. A. Logan, Radiative forcing of climate by changes in the vertical distribution of ozone, *J. Geophys. Res.*, *95*, 9971–9981, 1990.

Lelieveld, J., and F. J. Dentener, What controls tropospheric ozone?, *J. Geophys. Res.*, *105*, 3531–3551, 2000.

Lewis, A. C., and K. D. Bartle, A simplified method for the determination of atmospheric hydrocarbons, *LC-GC Int.*, *9*, 297–304, 1996.

Lewis, A. C., J. B. McQuaid, P. W. Seakins, M. J. Pilling, K. D. Bartle, and P. Ridgeon, Atmospheric monitoring of volatile organic compounds using programmed temperature vaporisation injection, *J. High Res. Chromatogr.*, *19*, 686–690, 1996.

Methven, J., Offline trajectories: Calculation and accuracy, *Tech. Rep. 44*, U.K. Univ. Global Atmos. Model. Programme, Dep. of Meteorol., Univ. of Reading, Reading, England, 1997.

Methven, J., M. Evans, P. Simmonds, and G. Spain, Estimating relationships between air-mass origin and chemical composition, *J. Geophys. Res.*, *106*, 5005–5019, 2001.

Monks, P., A review of observations and origins of spring ozone maximum, *Atmos Environ.*, *34*(21), 3545–3561, 2000.

Murphy, D. M., D. W. Fahey, M. H. Proffitt, S. C. Liu, K. R. Chan, C. S. Eubank, S. R. Kawa, and K. K. Kelly, Reactive nitrogen and its correlation with ozone in the lower stratosphere and upper troposphere, *J. Geophys. Res.*, *98*, 8751–8774, 1993.

Neuman, J. A., L. G. Huey, T. B. Ryerson, and D. W. Fahey, Study of inlet materials for sampling atmospheric nitric acid, *Environ. Sci. Technol.*, *33*, 1133–1136, 1999.

Penkett, S. A., and K. A. Brice, The spring maximum in photoxidants in the Northern Hemisphere troposphere, *Nature*, *319*, 655–657, 1986.

Pickering, K. E., R. R. Dickerson, G. J. Huffman, J. F. Boatman, and A. Schariot, Trace gas transport in the vicinity of frontal convective clouds, *J. Geophys. Res.*, *93*, 759–773, 1988.

U.K. Photochemical Oxidant Review Group (PORG), Fourth report of the Photochemical Oxidants Review Group, Dep. of the Environ., London, 1997.

Wayne, R. P., *Chemistry of Atmospheres: An Introduction to the Chemistry of the Atmospheres of Earth, the Planets, and Their Satellites*, Oxford Univ. Press, New York, 1996.

Zanis, P., P. S. Monks, E. Schuepbach, L. Carpenter, T. J. Green, G. P. Mills, S. Bauguitte, and S. A. Penkett, In situ ozone production under free tropospheric conditions during FREETEX '98 in Swiss Alps, *J. Geophys. Res.*, *105*, 24,223–24,234, 2000.

————————

S. R. Arnold, R. A. Carney, and J. B. McQuaid, School of the Environment, University of Leeds, Leeds LS2 9JT, UK.

H. Barjat, K. Dewey, and J. Kent, U.K. Meteorological Office, Farnborough GU14 0LX, UK.

N. Brough, S. A. Penkett, and C. E. Reeves, School of Environmental Sciences, University of East Anglia, Norwich NR4 7TJ, UK.

L. J. Carpenter, Department of Chemistry, University of York, York YO10 5DD, UK.

A. C. Lewis and R. M. Purvis, School of Chemistry, University of Leeds, Leeds LS2 9JT, UK. (allyl@chem.leeds.ac.uk)

J. Methven, Department of Meteorology, University of Reading, Reading RG6 6BB, UK.

P. S. Monks, School of Chemistry, University of Leicester, Leicester LE1 7RH, UK.